Current Indian Science

Content list available at: https://currentindianscience.com

RESEARCH ARTICLE

Catalytic Investigation of ε-caprolactone Polymerization through Schiff Base Titanium (IV) Complexes

Satyendra N. Shukla[1,*], Pratiksha Gaur[1], Dimple Deharia[1], Ripul Mehrotra[1], Sheela Mathews[1] and Vijay Chakrvarti[1]

[1]*Coordination Chemistry Research Lab, Department of Chemistry, Govt. Science (Autonomous) College, Jabalpur, 482001, MP, India*

Abstract:

Background:

The ring-opening polymerization (ROP) reaction has provided an efficient and convenient route to prepare polyesters of high molecular weight, low polydispersity index, and high optical purity. The poly(ε-caprolactone) (PCL) and poly(lactide) (PLA) were prepared through ROP reaction of ε-caprolactone and D, L-lactide, respectively. These compounds have a huge industrial demand and become an interest among the scientific community to develop more economically and eco-friendly catalysts for ROP reactions.

Methods:

Three Schiff base ligands, 2-((benzo[*d*]thiazole-2-ylimino)methyl)phenol, $\mathbf{L_1}$; **2**-(1-benzo[*d*]thiazole-2-ylimino)ethyl)phenol, $\mathbf{L_2}$; and 2-((benzo[*d*]thiazole-2-ylimino)methyl)-5-methoxyphenol, $\mathbf{L_3}$; were prepared by the reaction of 2-aminobenzothiazole with 2-hydroxybenzaldehyde, 2-hydroxyacetophenone and 2-hydroxy-4-methoxybenzaldehyde in 1:1 molar ratio. In anticipation of interesting stereochemistry, reactivity, and catalytic potential against ε-caprolactone polymerization, three Titanium(IV) complexes (**1 – 3**) of these Schiff base ligands were synthesized. All the prepared compounds were characterized by elemental analysis, molar conductance, FT-IR, UV-Vis, ^{1}H-NMR, ^{13}C{^{1}H}-NMR and FAB-Mass spectroscopic technique. Geometry was optimized with the help of DFT.

Results:

Complex **3** gives a much higher yield (87.7%) in comparison to **1** and **2**. The order of catalytic efficiency for complexes is **3**>**1**>**2**. With the increase in temperature, the % yield was found to decrease, and results are in support of moderate to good potency of synthesized catalysts.

Conclusion:

Complexes were screened for catalytic potency against ε-Caprolactone polymerization reaction. A most plausible mechanism for the polymerization was also proposed.

Keywords: ε-caprolactone, Catalytic activity, Polymerization, Schiff base, Titanium (VI), ROP.

Article History	Received: February 26, 2024	Revised: May 04, 2024	Accepted: May 29, 2024

1. INTRODUCTION

The biodegradable, biocompatible and permeable nature towards solvents for aliphatic polyesters *viz.* poly(ε-caprolactone) (PCL), poly(lactide) (PLA), and their copolymers made them an attractive option for a wide range of applications [1 - 3]. Its synthetic procedure under ring-opening polymerization (ROP) reaction has been subsequently studied in the recent past [4 - 9]. The potential application of titanium compounds was accepted and investigated by many scientists due to their stability under high oxidation states with polyanionic ligands. In this regard, the Salen type of ligands (bis(iminophenol)) and the donor framework around the metal ion where the two nitrogen atoms can be altered are the thrust of the current investigation [10].

The present communication discusses synthesis, spectroscopic characterization and the catalytic investigation of its titanium (IV) Schiff base complexes containing –*N*, *O* donor ligands. Geometry was also optimized with the help of DFT.

2. MATERIALS AND METHODS

2.1. Chemicals

AR grade 2-aminobenzothizole, salicylaldehyde, *o*-hydroxyacetophenone, acetophenone, sodium hydroxide, titanium tetrachloride (E. Merck) and ε-caprolactone (Himedia) were used as received. All the routine solvents, MeOH, EtOH,

* Address correspondence to this author at the Coordination Chemistry Research Lab, Department of Chemistry, Govt. Science (Autonomous) College, Jabalpur, 482001, MP, India; Tel: +91 9424657148; E-mails: sns1963_1@rediffmail.com, ccrl_2004@rediffmail.com

AcCN, acetone, DMSO, THF, and DCM, were dried and stored following standard procedure.

2.2. Instrumental Method

The CHN was estimated on Elementra Vario EL III, an elemental analyzer, and the melting point of the synthesized compound was determined by an open-capillary method on a digital melting point apparatus. Electronic absorption spectra were recorded with a Systronics 2201 UV-VIS double-beam spectrophotometer equipped with a PC. Conductivity measurements were carried out at 25 C on an EI-181 digital conductivity bridge with a dipping-type cell. FT-IR spectra were recorded in KBr pellets on a Shimadzu-8400 PC FT-IR spectrophotometer. The NMR experiments ^{1}H-^{13}C{^{1}H}-NMR were recorded in DMSO-d^6 and $CDCl_3$-d^1 on a DRX-400MHz Bruker. Fast atom bombardment-mass spectra (FAB-Mass) were recorded on a (JMS SX-102) Jeol Mass spectrometer using NBA as a matrix.

2.3. DFT Calculations

Gaussian-09 software package was employed to carry out all the quantum chemical calculations [11]. To understand the structural characteristics and vibrational properties of the ligands and their complexes density functional theory (DFT) method of B3LYP with 6-311++G(d,p) (without solvent) and/or 3-21+G* basic set for all nonmetallic atoms and Los Alamos National Laboratory 2 double zeta (LANL2DZ) basic set for the central metal atoms in the gas phase was used. The DFT calculations were performed using the B3LYP parameter, which includes Becke's gradient exchange correction with the Lee, Yang, and Parr correlation functional [12]. Optimized structural parameters of the compounds, such as bond lengths, bond angles and dihedral angles, were calculated with the atom numbering scheme of the molecule. The energy of the HOMO, LUMO levels, energy gap, absolute hardness (η), energies (ΔE), absolute softness (σ), global softness (S), chemical potential (Pi), electronic charge (ΔN_{max}), dipole moment (μ), global electrophilicity (ω), total energy (E-TD-HF/ETD-KS) and Mulliken electronegativity (χ) have been determined [13].

2.4. Catalytic Activity

Schiff base ligands and complexes were elucidated for their catalytic potency in ring-opening polymerization of ε-caprolactone [14, 15].

3. EXPERIMENTAL

3.1. Synthesis of Schiff Base Ligands

To the ethanolic solution (15 mL) of 2-aminobenzothiazole (0.01 moL), solution of aldehydes (0.01 moL), salicylaldehyde (in $\mathbf{L_1}$), 2-hydroxyacetophenone (in $\mathbf{L_2}$), 2-hydroxy-4-methoxybenzaldehyde (in $\mathbf{L_3}$) in 15 mL EtOH was added and kept under reflux for ~ 25 h. The solids started separating, were filtered off, washed with cold EtOH and dried under vacuum. The crude obtained was re-crystallized from a hot MeOH:H_2O mixture (4:1, *v/v*), resulting in shiny microcrystals.

3.1.1. 2-((Benzo[d]thiazole-2-ylimino)methyl)phenol, L_1

Colour = brown, Yield: 1.78 g (75.64%); m.p. = 120°C. $C_{14}H_{10}N_2OS$ (Mτ = 254.05) Anal. Calc. Required: C, 66.12; H, 3.96; N, 11.02%. Found: C, 66.09; H, 3.91; N, 10.98%. UV-Vis (ε in Lmol^{-1}cm^{-1}) in DMSO: 280(815), 380(1256). Selected infrared absorptions (KBr, cm^{-1}): ν(O-H) 3281 (m), ν(-CH=N) 1616(s), ν(C-O)1217(s), ν(C-S-C) 754. ^{1}H-NMR (DMSO-d^6, 400 MHz) spectra (δ value in ppm): δ(Ar-OH), 11.95(s, 1H); δ(CH=N), 9.07(s, 1H); δ(Ar-H)$_{Btz}$,7.06-7.21(m, 4H); δ(Ar-H)$_{phenolic}$, 7.25-7.48(m, 2H), 6.88(dd, 2H). ^{13}C-NMR spectra (δ value in ppm): δ(S-C-N), 180.1; δ(C-OH), 173.8; δ(CH=N), 162.1; δ(Ar-C)$_{phenol}$, 151.9-134.4; δ(Ar-C)$_{Btz}$, 128.0-116.4; ESI-Mass spectrum *m/z*, $[C_{14}H_{10}N_2OS+H]^+$ = 255.05, $[C_7H_6NO]^+$ = 120.04, $[C_7H_4NS+H]^+$ = 134.17, $[C_7H_4NS+H]^+$ = 237.29.

3.1.2. 2-(1-Benzo[d]thiazole-2-ylimino)ethyl)phenol, L_2

Colour = yellow, Yield: 1.76 g (78.24%); m.p. = 110°C. $C_{15}H_{12}N_2OS$ (Mτ = 268.33) Anal. Calc. Require: C, 67.14; H, 4.51; N, 10.44%. Found: C, 67.10; H, 4.48; N, 10.40%. UV-Vis (ε in Lmol^{-1}cm^{-1}) in DMSO: 250(398), 360(3412). Selected infrared absorption (KBr, cm^{-1}): ν(O-H), 3263(m); ν(-CH=N), 1612(s), ν(C-O), 1236(s); ν(C-S-C), 756. ^{1}H-NMR (DMSO-d^6, 400 MHz) spectra (δ value in ppm): δ(Ar-OH), 11.96(s, 1H); δ(Ar-H)$_{Btz,}$,7.06-7.20(m, 4H); δ(Ar-H)$_{phenolic}$, 7.25-7.47(m, 2H), 6.88(dd, 2H). ^{13}C-NMR spectra (δ value in ppm): δ(S-C-N), 179.8; δ(C-OH), 172.9; δ(CH=N), 162.1; δ(Ar-C)$_{phenolq}$, 150.1-132.1; δ(Ar-C)$_{Btz}$, 127.4-117.1; δ(-CH_3), 26.3. ESI-Mass spectrum *m/z*, $[C_{15}H_{12}N_2OS+H]^+$ = 269.33, $[C_8H_8NO]^+$ = 134.06, $[C_9H_7N_2S+H]^+$ = 175.03, $[C_{15}H_{11}N_2S+H]^+$ = 251.06. $[C_{14}H_9N_2OS+H]^+$ = 253.04.

3.1.3. 2-((Benzo[d]thiazole-2-ylimino)methyl)-5-methoxy-phenol, L_3

Colour = orange, Yield: 2.56 g (85.48%); m.p. = 120°C. $C_{15}H_{12}N_2O_2S$ (Mτ = 284.33) Anal. Calc. Require: C, 63.36; H, 4.25; N, 9.85%. Found: C, 63.32; H, 4.21; N, 9.81%. UV-Vis (ε in Lmol^{-1}cm^{-1}) in DMSO: 260(463), 340(3298). Selected infrared absorption (KBr, cm^{-1}): ν(O-H) 3262 (m), ν(-CH=N) 1624(s), ν(C-O)1224(s), ν(C-S-C) 755. ^{1}H-NMR (DMSO-d^6, 400 MHz) spectra (δ value in ppm): δ(Ar-OH), 11.95(s, 1H); δ(CH=N), 9.102(s, 1H); δ(Ar-H)$_{Btz}$,7.07-7.20(m, 4H); δ(Ar-H)$_{phenolic}$, 7.25-7.47(m, 2H), 6.88(dd, 2H); δ(OCH_3), 3.57(s, 3H). ^{13}C-NMR spectra (δ value in ppm): δ(S-C-N), 179.75; δ(C-OH), 173.45; δ(CH=N), 161.86; δ(Ar-C)$_{phenol}$, 153.15-133.15; δ(Ar-C)$_{Btz}$, 128.24-114.28; δ(OCH_3), 60.17. ESI-Mass spectrum *m/z*, $[C_{15}H_{12}N_2O_2S+H]^+$ = 285.33, $[C_7H_4NS]^+$ = 134.00, $[C_8H_8NO_2]^+$ = 150.05, $[C_{14}H_9N_2OS+H]^+$ = 253.04. $[C_{15}H_{11}N_2OS+H]^+$ = 267.05, $[C_{14}H_9N_2O_2S+H]^+$ = 269.03.

3.2. *Synthesis of Complexes* (1 – 3)

The $TiCl_4$ (0.001 mol) was dissolved in 10 mL of THF and added slowly (drop by drop) to the solution of Schiff base ligands ($\mathbf{L_1}$ – $\mathbf{L_3}$, 0.001 mol) prepared in 10 mL THF. The mixture was kept under stirring at room temperature for 2 h under the stream of nitrogen. The solid precipitates were filtered and washed several times with acetone:water (1:1, *v/v*)

solvent mixture. The crude obtained was re-crystallized with ethanol and dried under vacuum.

3.2.1. [Ti(L$_1$)(H$_2$O)Cl$_3$], 1

Color = black, Yield: 59.25%; m.p. > 300 °C; Anal. Calc. $C_{14}H_{11}Cl_3N_2O_2STi$ (Mτ = 425.54): Require: C, 39.51; H, 2.61; N, 6.58. Found: C, 39.14; H, 2.55; N, 6.44. Λ_m at 25C (Ω^{-1} cm^2 mol^{-1}): 3.0 in DMSO. UV-Vis (λ_{max}, nm (ε in Lmol^{-1}cm^{-1}) in DMSO: 300(6583), 440(3232). Selected infrared absorption (KBr, cm^{-1}): ν(-CH=N), 1608(s); ν(C-O), 1202(s); ν(M-O), 576(s); ν(M-N), 489(s); ν(C-S-C), 752. ^{1}H-NMR (DMSO-*d*^{6}, 400 MHz) spectra (δ value in ppm): δ(CH=N), 8.97(s, 1H); δ(Ar-H)$_{Btz}$,7.83-7.99(m, 4H); δ(Ar-H)$_{phenolic}$, 8.82-9.00(m, 4H). δ(OH)$_{H2O}$, 5.10(s, 2H). ^{13}C-NMR spectra (δ value in ppm): δ(S-C-N), 179.1; δ(C-OH), 172.7; δ(CH=N), 155.3; δ(Ar-C)$_{phenol}$, 151.8-133.1; δ(Ar-C)$_{Btz}$, 128.4-115.8. ESI-Mass spectrum *m/z*, $[C_7H_6Cl_3NO_3Ti+H]^+$ = 304.88, $[C_{14}H_{10}Cl_3N_2O_3STi+H]^+$ = 438.89, $[C_{14}H_{10}Cl_3N_2O_3STi+H]^+$ = 441.53.

3.2.2. [Ti(L$_2$)(H$_2$O)Cl$_3$], 2

Color = red, Yield: 56.48%; m.p. > 300 °C; Anal. Calc. $C_{15}H_{13}Cl_3N_2O_2STi$ (Mτ = 439.57): Require: C, 40.99; H, 2.98; N, 6.37. Found: C, 40.59; H, 2.89; N, 6.42. Λm at 25C (Ω^{-1} cm^2 mol^{-1}): 07 in DMSO. UV-Vis (λmax, nm (ε in Lmol^{-1}cm^{-1}) in DMSO: 285(1409), 460(1523). Selected infrared absorption (KBr, cm^{-1}): ν(-CH=N), 1597(s); ν(C-O), 1214(s); ν(M-O), 570(s); ν(M-N), 462(s); ν(C-S-C), 753. ^{1}H-NMR (DMSO-*d*^{6}, 400 MHz) spectra (δ value in ppm): δ(Ar-H)$_{Btz}$, 7.84-7.98(m, 4H); δ(Ar-H)$_{phenolic}$, 8.83-9.00 (m, 4H); δ(OH)$_{H2O}$, 5.12(s, 2H); δ(-CH$_3$), 2.86(s, 3H). ^{13}C-NMR spectra (δ value in ppm): δ(S-C-N), 177.4; δ(C-OH), 169.5; δ(Ar-C)$_{phenol}$, 151.1-133.5; δ(Ar-C)$_{Btz}$, 128.4-120.1; δ(-CH$_3$), 25.5. ESI-Mass spectrum *m/z*, $[C_8H_8Cl_3NO_3Ti+H]^+$ = 318.90, $[C_{15}H_{11}Cl_3N_2OSTi+H]^+$ = 419.91, $[C_{14}H_9Cl_3N_2O_3STi+H]^+$ = 437.88, $[C_{15}H_{12}Cl_3N_2O_3STi+H]^+$ = 455.55.

3.2.3. [Ti(L$_3$)(H$_2$O)Cl$_3$], 3

Color = black, 66.52%; m. p. >300 °C; Anal. Calc. $C_{15}H_{13}Cl_3N_2O_3STi$ (Mτ = 455.57): Require: C, 39.55; H, 2.88; N, 6.15. Found: C, 39.26; H, 2.58; N, 5.91. Λm at 25C (Ω^{-1} cm^2 mol^{-1}): 04 in DMSO. UV-Vis (λmax, nm (ε in Lmol^{-1}cm^{-1}) in DMSO: 320(1968), 440(1685). Selected infrared absorption (KBr, cm^{-1}): ν(-CH=N), 1603(s); ν(C-O), 1208(s); ν(M-O), 584(s); ν(M-N), 436(s); ν(C-S-C), 751. ^{1}H-NMR (DMSO-*d*^{6}, 400 MHz) spectra (δ value in ppm): δ(CH=N), 8.96(s, 1H); δ(Ar-H)$_{Btz}$,7.84-7.98(m, 4H); δ(Ar-H)$_{phenolic}$, 7.26-7.48(m, 2H). δ(OH)$_{H2O}$, 5.11(s, 2H); δ(-OCH$_3$), 3.562(s, 3H). ^{13}C-NMR spectra (δ value in ppm): δ(S-C-N), 183.1; δ(C-OH), 174.5; δ(CH=N), 152.5; δ(Ar-C)$_{phenol}$, 150.1-131.5; δ(Ar-C)$_{Btz}$, 128.4-116.2; δ(OCH$_3$), 60.0. ESI-Mass spectrum *m/z*, $[C_{14}H_8Cl_3N_2O_3STi+H]^+$ = 436.88, $[C_{14}H_8Cl_3N_2O_4STi+H]^+$ = 452.87, $[C_{15}H_{12}Cl_3N_2O_4STi+H]^+$ = 468.89, $[C_{15}H_{12}Cl_3N_2O_4STi+H]^+$ = 471.56.

3.3. Ring-opening Polymerization (ROP) of ε-caprolactone

The ring opening polymerization of ε-caprolactone was investigated over different ranges of synthesized titanium complexes (**1 – 3**, 0.1 mmol), with variations in temperature and time [16]. In brief, a mixture of ε-caprolactone (0.97 mL, 8.8 mmol) and the prepared titanium catalyst was taken in an R. B. flask and kept on heating (in a muffle furnace) over the different temperature ranges (100, 125 and 150 ºC). The observations were also recorded at 6, 12 and 24 h time duration for each set of the synthesized complex. After the completion of the reaction, the resulting crude was dissolved in 10 mL of $CHCl_3$ and centrifuged at 300 rpm for ~ 5 minutes. The obtained solution was poured into a beaker filled with an excess of MeOH (~ 20 mL). The white solid started separating out, which was recovered by filtration, washed with MeOH and dried overnight under vacuum. Mw = 33,000; IR (KBr): Selected infrared absorption (KBr, cm^{-1}): ν(C=O) 1727(s), ν(-CH$_2$) 2864(s), 2942(s); ν(-OH) 3433. ^{1}H-NMR ($CDCl_3$-*d*^{1}, 400 MHz) spectra (δ value in ppm): *δ* 2.30(*t*, 2H, -CH$_2$), *δ* 1.65(*m*, 2H, -CH$_2$), *δ* 1.40(*m*, 2H, -CH$_2$), *δ* 4.40(*t*, 2H, -CH$_2$).

4. RESULTS AND DISCUSSION

4.1. Quantum Chemical Calculations

The quantum chemical parameters, E_{HOMO}, E_{LUMO} the difference between HOMO and LUMO energy levels (ΔE), Mulliken electronegativity (χ), dipole moment, chemical potential (μ or Pi), global hardness (η), global softness (S), global electrophilicity (ω), absolute softness (σ) and electronic charge (ΔN_{max}) have been elucidated and presented in Table **1**. The highest occupied molecular orbital (E_{HOMO}) and the lowest unoccupied molecular orbital (E_{LUMO}) are the main descriptors of chemical stability. The HOMO represents the ability to donate an electron and LUMO in an electron acceptor [17]. The value of the energy gap (ΔE) is high in $\mathbf{L_2}$, which indicates less reactivity of the ligands. In complexes ΔE is highest in

Table 1. Calculated quantum chemical parameters of L_1 - L_3 and complex 1 – 3.

Ligands / Complexes	HOMO	LUMO	ΔE	Mulliken Electronegativity, χ	Global Hardness, η	Absolute Softness, σ	Chemical Potential, μ	Global Softness, S	Global Electrophilicity, ω	Electronic Charge, ΔN	Dipole Moment, μ	E(TD-HF/TD-KS)
L_1	-3.844773	-0.94146	2.90331	2.3931195	1.451654	0.68887	-2.39312	0.3444388	1.972585	1.648547	2.7927	-1122.3538
L_2	-5.9423919	-2.17788	3.7645	4.0601402	1.882252	0.531279	-4.06014	0.2656393	4.378993	2.157065	4.5504	-1161.4642
L_3	-5.5668939	-1.90415	3.66274	3.7355249	1.831369	0.54604	-3.735525	0.2730198	3.809758	2.039744	4.0567	-1275.9481
1	-6.7663107	-3.82028	2.94603	5.2932974	1.473013	0.67888	-5.293297	0.3394402	9.510774	3.593516	11.2861	-913.14437
2	-5.9666088	-3.36614	2.60046	4.666379	1.30023	0.769095	-4.666379	0.3845474	8.373555	3.588887	9.2137	-952.19355
3	-4.9010652	-3.50464	1.39642	4.2028566	0.698209	1.432237	-4.202857	0.7161184	12.64951	6.019485	8.2510	-1066.4110

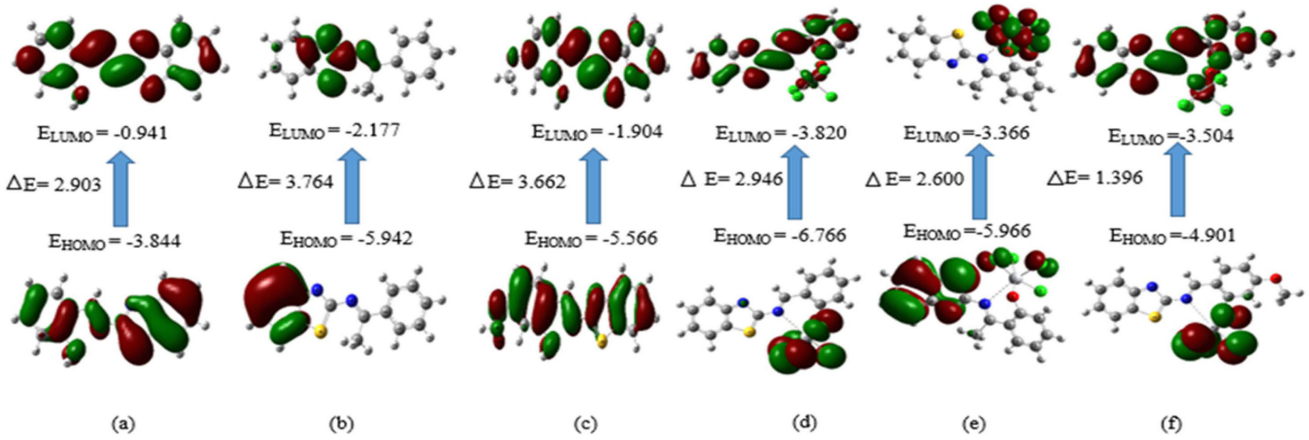

Fig. (1). HOMO-LUMO and energy difference of (**a**) L_1 (**b**) L_2 (**c**) L_3 (**d**) Complex **1 (e)** Complex **2** and (**f**)Complex **3** .

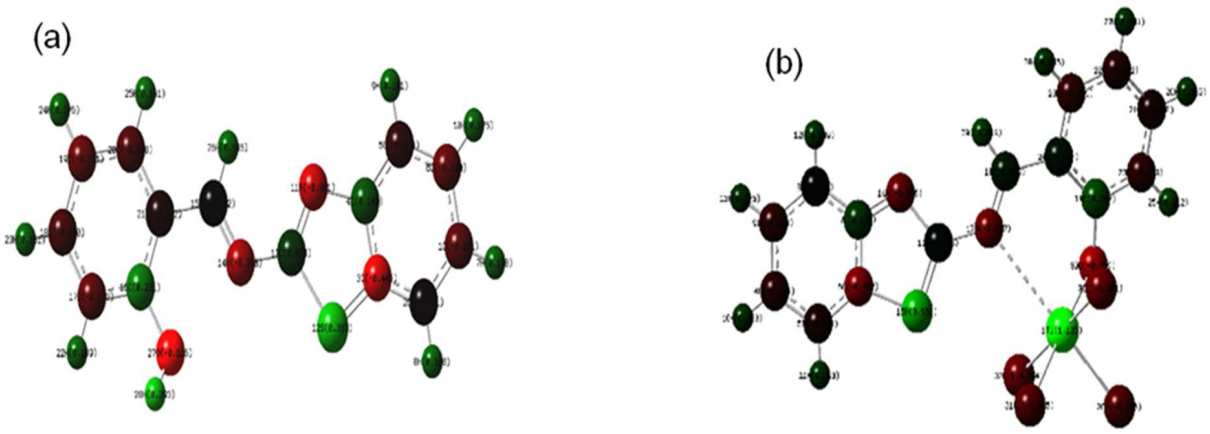

Fig. (2). Mulliken atomic charge plot of (**a**) L_1 and (**b**) complex **1**.

complex **1** and lowest in complex **3,** which indicates higher stability and low reactivity of complex **1** and lower stability and more reactivity of complex **2**. The E_{LUMO} values were low in L_2**,** which is an indicator of its low affinity for electrons. The E_{LUMO} values were almost the same in complexes. The high value of E_{HOMO} was observed in L_1**,** which may be due to its powerful donation behaviour. Global hardness (η) and absolute softness (σ) parameters are indicators of molecular stability and reactivity. The negative data of both E_{LUMO} and E_{HOMO} were attributed to the stability of complexes [18] (Fig. **1**).

4.1.1. Mulliken Atomic Charge Analysis

The net atomic charges of ligands and complexes were obtained utilizing Mulliken population analysis. Charge distribution on a molecule has a significant influence on the vibrational spectra [19]. This calculation depicts the charges of every atom in the molecule. The distribution of positive and negative charges is the major reason for the increase or decrease in the bond length. The comparative values of both scales for L_1 and complex **1** are represented in the O and N atoms, showing that these atoms bear a negative charge and exhibit donating properties. Hydrogen atoms of L_1 and metal atoms of complex **1** displayed positive charges and exhibited electron-accepting properties [20]. Mulliken atomic charge plot and pattern of ligand L_1 and complex **1** are displayed in Fig. (**2a** and **b**).

4.1.2. Molecular Electrostatic Potential Analysis (MEP)

The MEP is related to the electronic density and is a very useful descriptor in the understanding of electron-rich and electron-deficient sites as well as H-bonding interactions. As it can be easily observed from the MEP map of the ligands and complexes, that molecule has several potential sites for coordination. The negative regions are mainly over the oxygen atoms (deep red/yellow) on each of the O-H groups and nitrogen atoms of the imine groups. The hydrogen and carbon atoms bear the maximum region of positive charge, and the most positive regions (blue/green) are observed around the hydrogen atoms of phenolic O–H groups as well as carbon atoms of azomethine groups. In ligand, the highest range was observed as -7.880(10-3 au) and +7.880(10-3 au in L3). However, in complexes, the highest range was observed as

-9.605×10^{-3} au to $+9.605\times10^{-3}$ au in complex **1.** The nitrogen atoms and the oxygen atoms are negative sites. Different colours represent the different values of the electrostatic potential at the surface. The potential increases in the order: **Red < Orange < Yellow < Green < Blue** [21]. The MEP maps of all compounds are shown in Fig. (**3**).

4.1.3. Bond Parameters

DFT calculated the optimized bond lengths and bond angles of the investigated compound following the atom numbering scheme shown in Table **2**. The optimized geometrical parameters of ligands are compared with complexes. The bond length of azomethine >C=N in ligands was ~1.33 Å, which increased in the case of complexes and was observed at ~1.38 Å. This increase in bond distance was because of the transfer of electron density of the double bond towards metal and the decrease in the double bond character of >C=N, which in turn confirms the coordination of metal with azomethine-N. The calculated C-O bond distance in complexes was observed at ~1.44 Å, which was slightly longer than free ligands. From the data, it was observed that the geometry of complexes was slightly distorted from octahedral and bond angles and distances slightly deviated.

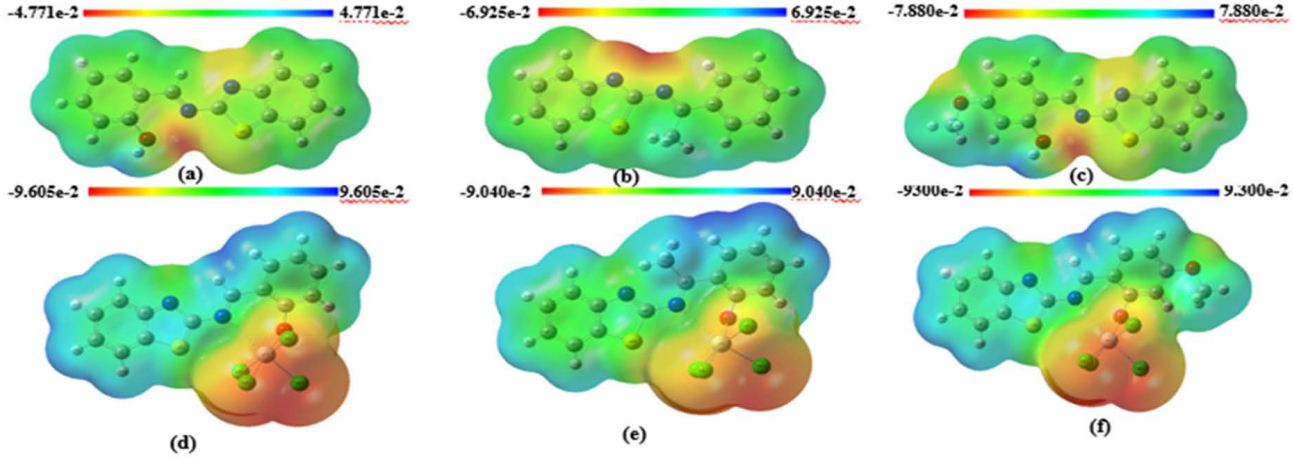

Fig. (3). MEP maps of(**a**) L_1 (**b**) L_2 (**c**) L_3 (**d**) Complex **1** **(e)** Complex **2** and(**f**)Complex **3** .

Table 2. Selected geometrical bond length of ligands and complexes.

Bond Connectivity	Bond Length (in A°)					
	L_1	L_2	L_3	Complex 1	Complex 2	Complex 3
C-N benzothiazole	(C23-N21) 1.4712	(C23-N21) 1.4701	(C22-N20) 1.4734	(C23-N21) 1.47950	(C23-N21) 1.47010	(C22-N20) 1.47034
N=C (azomethine)	(C25= N21) 1.3377	(C25= N21) 1.3379	(C24= N20) 1.3378	(C25= N21) 1.38652	(C25= N21) 1.38413	(C24= N20) 1.38496
C-O	(C15-O27) 1.4303	(C15-O26) 1.4310	(C15-O25) 1.4307	(C15-O27) 1.4416	(C15-O26) 1.4476	(C15-O25) 1.4437
C-O′	-	-	-	-	-	(C11-O37) 1.44006
O-H	(O27-H28) 0.9600	(O26-H27) 0.9610	(O25-H30) 0.9601	-	-	-
C-C	-	(C25-C28) 1.5420	(C24-C26) 1.5408	-	(C15-C26) 1.5144	(C24-C23) 1.5401
C-C′	-	-	-	-	-	-
C-H	(C25-H26) 1.0700	-	-	(C25-H26) 1.0823	-	-
N-Ti	-	-	-	(N21-Ti28) 2.0279	(N21-Ti27) 2.0141	(N21-Ti27) 2.0149
N-Ti′	-	-	-	-	-	-
O-Ti	-	-	-	(O27-Ti28) 1.99955	(O26-Ti27) 2.00294	(O26-Ti25) 1.97735
O-Ti′	-	-	-	(O32-Ti28) 1.8962	(O31-Ti27) 1.9976	(O26-Ti30) 1.9820
Ti-Cl	-	-	-	(Ti28-Cl31) 2.36070	(Ti27-Cl28) 2.32157	(Ti26-Cl27) 2.31077
Ti-Cl’	--	-	-	(Ti28-Cl30) 2.35270	(Ti27-Cl29) 2.29768	(Ti26-Cl28) 2.30775
Bond angle (in degree radian)						
<C-C-H	<C14-C25-H26 120.0000	-	-	-	-	-

(Table 2) contd.....

Bond Connectivity	Bond Length (in A°)					
	L_1	L_2	L_3	Complex 1	Complex 2	Complex 3
<C-C-C	-	<C14-C25-C28 120.0000	<C14-C24-C26 119.9999	<C25-C14-C15 124.1483	<C14-C25-C34 119.5880	<C14-C24-C33 118.3004
<C-O-H	<C15-O27-H28 109.4712	<C15-O26-H27 109.4720	<C15-O25-H30 109.4718	-	-	-
(<C-N-C)	<C25-N21-C23 119.9999	<C25-N21-C23 119.9998	<C24-N20-C22 119.9995	<C23-N21-C25 117.7714	<C25-N21-C23 119.1445	<C24-N20-C22 118.7807
(<C-O-C)	-	-	<C11-O31-C32 109.4712	-	-	<C11-O37-C38 109.5361
<C-O-M	-	-	-	<C15-O27-Ti28 112.3944	<C15-O26-Ti27 114.5249	<C15-O25-Ti26 116.9012
<O-M-O	-	-	-	<O27-Ti28-O32 96.4467	<O26-Ti27-O31 89.7088	<O25-Ti26-O30 89.2807

4.2. Spectral Characterization of Ligands and Complexes

The CHN data of the synthesized ligands were in agreement with the stoichiometries. Molar conductance of **1 – 3** was between 3 - 9 $\Omega^{-1}cm^2mol^{-1}$, indicating the non-electrolytic nature of complexes [22]. ESI-MS spectrum of ligands exhibits several peaks due to fragmentation. The pseudo molecular ion peak observed at *m/z* 255 in $\mathbf{L_1}$, 269 in $\mathbf{L_2}$ and 285 in $\mathbf{L_3}$ attributed to a molecular fragment indicates the molecular mass of the ligand. Several other peaks for various fragments were also obtained [23]. The complexes also displayed several peaks, including a pseudomolecular ion peak for [M+H+]+, which was inevitably present in each case.

4.2.1. FT-IR Spectral Studies

A strong peak appeared between 1612 to 1624 cm^{-1} in the $\mathbf{L_1 - L_3}$, assigned for imine ν(HC=N–) group, was found to shift downwards in **1 – 3**, confirming the coordination of azomethine nitrogen to the metal [23 - 25]. A weak band observed at ~ 3262 cm^{-1} due to ν(O–H) vibrations was found absent in complexes, and the peak of medium intensity (appeared around 570 cm^{-1}, assigned for M–O bond), confirms deprotonation of the phenolic group in coordination [26].

4.2.2. Electronic Spectral Study

UV–Vis spectra of ligands exhibit two absorption bands at ~280 nm and ~380 nm. The first band of low molar extinction was assigned to π→ π* transition associated with the aromatic ring. Another band of high intensity, at ~380 nm, was attributed to n→ π* transition for the -HC=N group [27]. Complexes are diamagnetic, as expected for Ti(IV) metal ions. The electronic spectra of complexes exhibit only two bands at ~300 nm and 440 nm ascribed for π→ π* and n→ π*, respectively [28]. The band of medium intensity at ~ 440 nm was shifted from those observed in ligands. Shifting of this band to a higher wavelength indicates the transfer of electron pair from azomethine-N to metal [29].

4.2.3. NMR Spectral Studies

In the ^{1}H-NMR spectrum, a singlet at ~ δ 11.9 ppm in $\mathbf{L_1 - L_3}$ was assigned for phenolic hydrogen and was found to disappear in **1 – 3** due to the involvement of phenolic-OH in coordination with metal. The sharp singlet ascribed for the azomethine proton in $\mathbf{L_1}$ and $\mathbf{L_3}$ was shifted to the lower field in **1** and **3** and appeared at ~ δ 8.9 ppm, indicating binding of Schiff Base ligand to metal by donating lone pair from azomethine nitrogen to the metal. In ^{13}C-NMR spectra of L1 – L3, the signal observed at *δ* 162.1 ppm for azomethine carbon was shifted to the lower field and appeared at about *δ* 153 ppm, indicating coordination of Schiff Base ligand to metal by donating a lone pair from azomethine-N to metal [23, 24]. In $\mathbf{L_{3,\ the}}$ presence of the methoxy group was ascertained by a singlet at δ 3.57 ppm [30]. The singlet at ~ δ 5 ppm in the ^{1}H-NMR spectrum of **1 – 3** was assigned for two coordinated water protons.

4.2.4. Proposed Structure for Ligands and Complexes

Based on molar conductance, elemental analyses, electronic spectral studies, infrared, NMR, Mass and DFT studies, the most probable structure for the ligands ($\mathbf{L_1 - L_3}$) complexes **1 – 3** was suggested in Fig. (**4**).

Table 3. Ring opening polymerization (ROP) of *ε*-caprolactone for complexes 1 – 3.

Complexes	ε-caprolactone (mmoL)	Catalyst (mmoL)	Temperature (°C)	Time (h)	% Yield
Complex 1	8.8	0.1	125	6	78.4
				12	78.9
				24	79.2
Complex 2	8.8	0.1	125	6	65.7
				12	66.5
				24	68.8
Complex 3	8.8	0.1	125	6	86.2
				12	87.7
				24	88.9

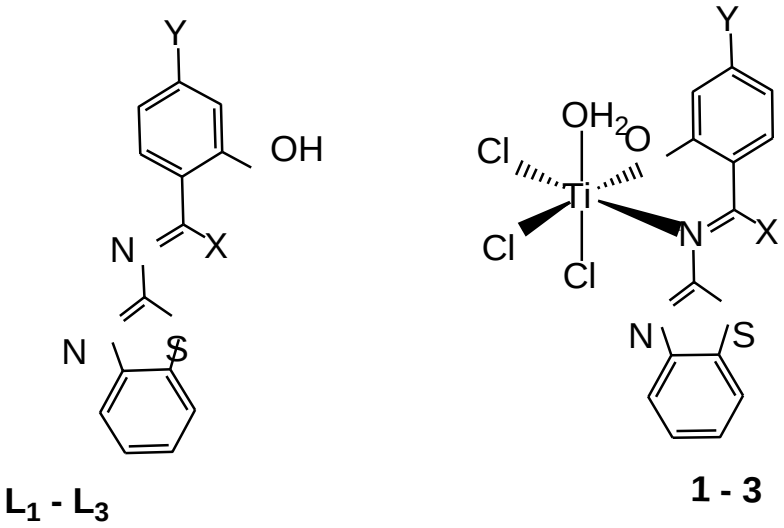

Fig. (4). Structure of Schiff base ligands and complexes. Where, X = H in L_1, L_3, **1** and **3**, and CH_3 in $L_2$and **2**; Y = H in L_1, L_2, **1** and **2**, and OCH_3 in L_3 and **3**.

4.3. Ring-opening Polymerization (ROP) of ε-caprolactone

The ring opening polymerization of ε-caprolactone was investigated over different ranges of synthesized titanium complexes (**1 – 3**, 0.1 mmol), with variations in temperature and time [16]. Results obtained are depicted in Table **3** and Figs. (**5** and **6**). Fig. (**5**) highlights the ring opening polymerization of ε-caprolactone at 0.1 mmoL of titanium catalyst **1 – 3**, at 125 ºC for 12 h. Complex **3** gives a much higher yield (87.7%) in comparison to **1** and **2**. Fig. (**4**) describes the % yield with variation in temperature at 0.1 mmol of **3** for 12 h. A fall was reported in % yield on increasing the temperature, while on increasing reaction, the jump in % yield was observed (Table **3**). From the data, it is clear that the order of catalytic efficiency of complexes is **3**>**1**>**2**. A most plausible mechanism for the polymerization was also proposed in Fig. (**7**).

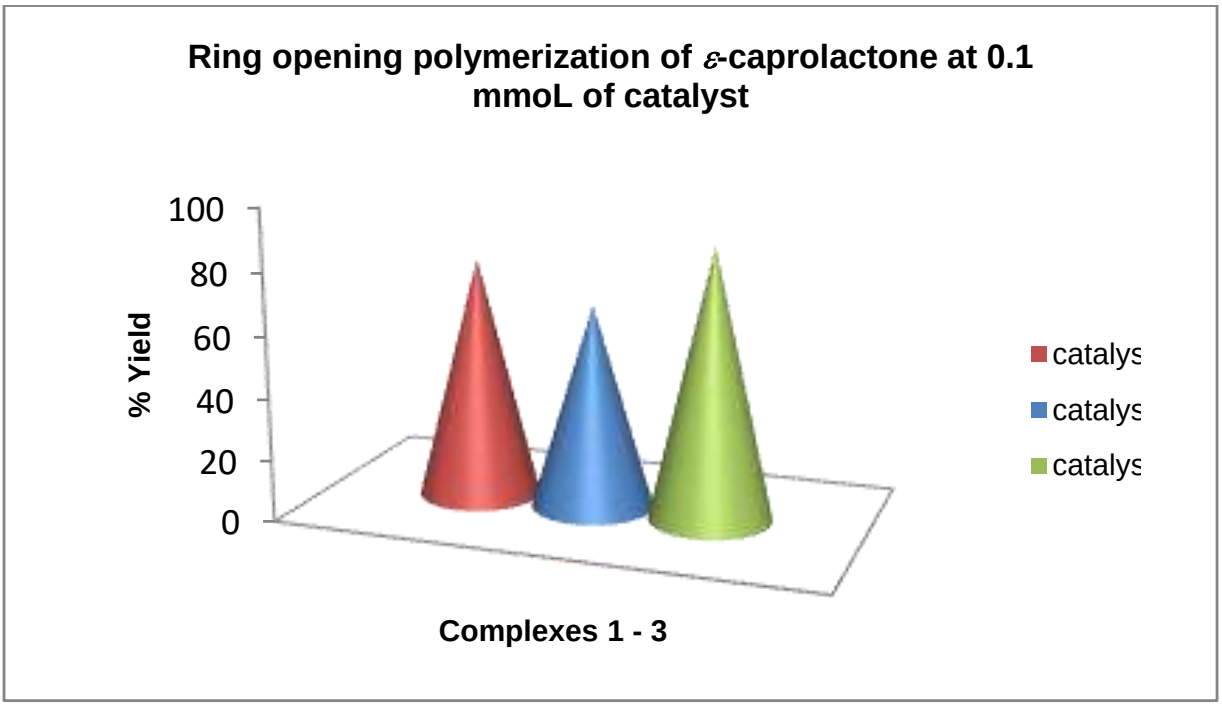

Fig. (5). Reaction condition: ε-caprolactone (0.97 mL, 8.8 mmoL), titanium complexes (**1 – 3**, 0.1 mmoL), Temperature 125 ºC, Time 12 h.

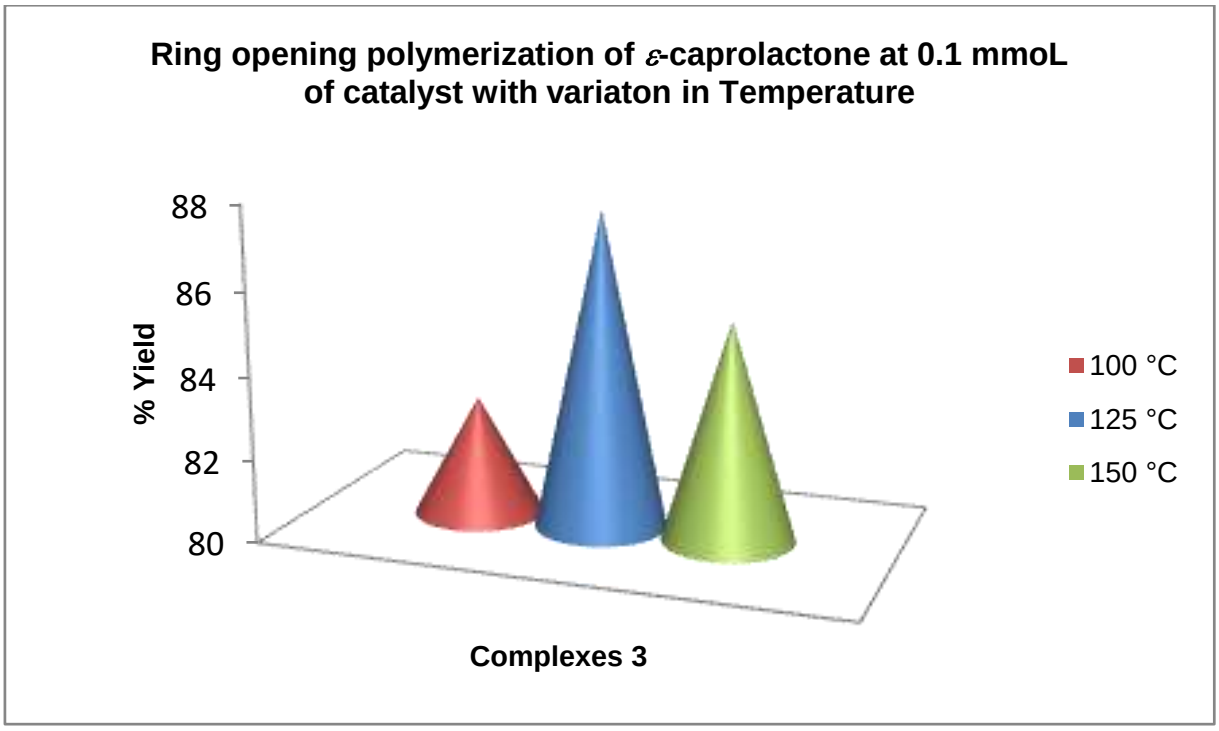

Fig. (6). Reaction condition: ε-caprolactone (0.97 mL, 8.8 mmoL), titanium complexes **3** (0.1 mmoL), Time 12 h.

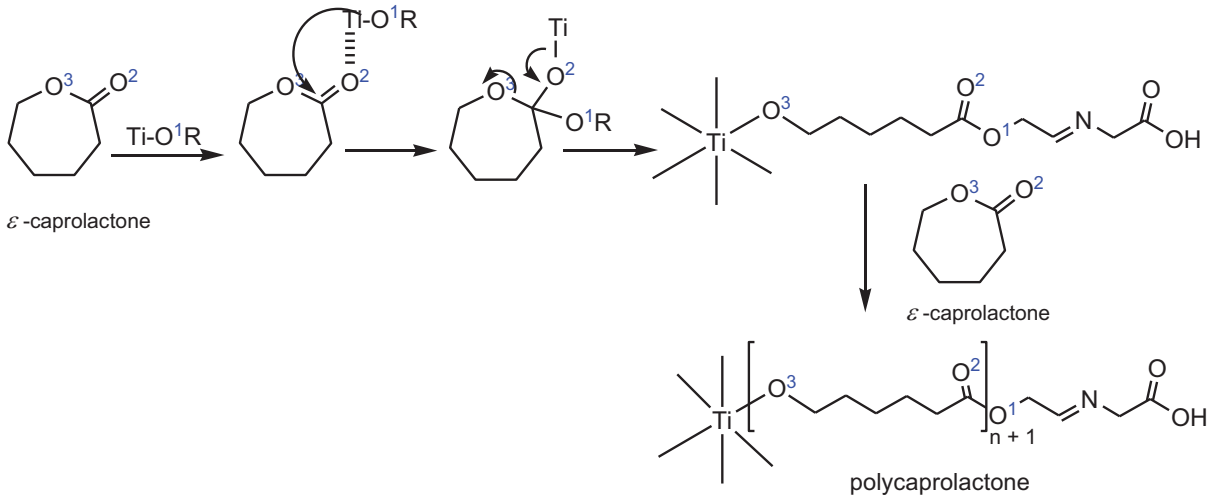

Fig. (7). A plausible mechanism for ring opening polymerization of ε-caprolactone.

CONCLUSION

In this study, three Schiff base ligands and their complexes were synthesized and characterized by various analytical techniques. Structure analysis reveals the formation of the complex *via* bidentate -*ON* donor ligands. A water molecule also participates in coordination with the metal centre along with three bonded –Cl, and confirmed with proton NMR spectral analysis. DFT was employed to get more insight into molecular structure. The difference in energy of HOMO and LUMO ΔE is high in complex **1**, indicating higher stability of complex **1** than others. Mulliken atomic charge analysis and Molecular Electrostatic Potential, MEP confirm the mode of coordination of metal *via N* and *O*. All three complexes were also examined against ring opening polymerization of ε-caprolactone under solvent-free conditions. Results support the moderate to good potency of synthesized catalysts.

AUTHORS' CONTRIBUTION

It is hereby acknowledged that all authors have accepted responsibility for the manuscript's content and consented to itssubmission. They have meticulously reviewed all results and unanimously approved the final version of the manuscript.

LIST OF ABBREVIATIONS

ROP	=	Ring-opening polymerization
PCL	=	Poly (ε-caprolactone)
PLA	=	Poly (lactide)

ETHICS APPROVAL AND CONSENT TO PARTICIPATE

Not applicable.

HUMAN AND ANIMAL RIGHTS

Not applicable.

CONSENT FOR PUBLICATION

Not applicable.

AVAILABILITY OF DATA AND MATERIALS

The data and supportive information are available within the article.

FUNDING

None.

CONFLICT OF INTEREST

Dr. Satyendra N. Shukla is the Associate Editorial Board Member of the journal Current Indian Science.

ACKNOWLEDGEMENTS

The authors would extend their acknowledgement to the Head, Department of Chemistry and Principal, Govt. Science (Autonomous) College, Jabalpur, for their constant support and encouragement during manuscript drafting.

REFERENCES

[1] Lemaire, M.; Mangeney, P. *Chiral diazaligands for asymmetric synthesis in topics in organometallic chemistry*; Springer- Verlag: Berlin, Heidelberg, **2005**, 15, pp. 1-20.

[2] Knight, P.; Scott, P. Predetermination of chirality at octahedral centres with tetradentate ligands: prospects for enantioselective catalysis. *Coord. Chem. Rev.,* **2003**, *242*(1-2), 125-143. [http://dx.doi.org/10.1016/S0010-8545(03)00067-5]

[3] Che, C.; Huang, J.S. Metal complexes of chiral binaphthyl Schiff-base ligands and their application in stereoselective organic transformations. *Coord. Chem. Rev.,* **2003**, *242*(1-2), 97-113. [http://dx.doi.org/10.1016/S0010-8545(03)00065-1]

[4] Repo, T.; Klinga, M.; Pietikäinen, P.; Leskelä, M.; Uusitalo, A.M.; Pakkanen, T.; Hakala, K.; Aaltonen, P.; Löfgren, B. Ethylenebis(salicylideneiminato)zirconium dichloride: crystal structure and use as a heterogeneous catalyst in the polymerization of ethylene. *Macromolecules,* **1997**, *30*(2), 171-175. [http://dx.doi.org/10.1021/ma960512r]

[5] Mason, A.F.; Coates, G.W. New phenoxyketimine titanium complexes: combining isotacticity and living behavior in propylene polymerization. *J. Am. Chem. Soc.,* **2004**, *126*(50), 16326-16327. [http://dx.doi.org/10.1021/ja044268s] [PMID: 15600326]

[6] Romain, C.; Brelot, L.; Bellemin-Laponnaz, S.; Dagorne, S. Synthesis and structural characterization of a novel family of titanium complexes bearing a tridentate bis-phenolate-N-heterocyclic carbene dianionic ligand and their use in the controlled ROP of *rac* -lactide. *Organometallics,* **2010**, *29*(5), 1191-1198. [http://dx.doi.org/10.1021/om901084n]

[7] Zhang, J.; Lin, Y.J.; Jin, G.X. Synthesis, characterization, and ethylene polymerization of group IV Metal complexes with Mono-Cp and tridentate aryloxide or arylsulfide ligands. *Organometallics,* **2007**, *26*(16), 4042-4047. [http://dx.doi.org/10.1021/om700338y]

[8] Bischoff, C.A.; Walden, P. Ueber das Glycolid und seine Homologen. *Ber. Dtsch. Chem. Ges.,* **1893**, *26*(1), 262-265. [http://dx.doi.org/10.1002/cber.18930260158]

[9] Farrar, D.; Bioresorbable Polymers, B.B. in Orthopaedics. *Med. Device Manuf. Technol,* **2005**, *1*, 4.

[10] Saha, T.K.; Ramkumar, V.; Chakraborty, D. Salen complexes of zirconium and hafnium: synthesis, structural characterization, controlled hydrolysis, and solvent-free ring-opening polymerization of cyclic esters and lactides. *Inorg. Chem.,* **2011**, *50*(7), 2720-2722. [http://dx.doi.org/10.1021/ic1025262] [PMID: 21370885]

[11] Frisch, M.J.; Trucks, G.W.; Schlegel, H.B.; Scuseria, G.E.; Robb, M.A.; Cheeseman, J.R.; Scalmani, G.; Barone, V.; Mennucci, B.; Petersson, G.A.; Nakatsuji, H.; Caricato, M.; Li, X.; Hratchian, H.P.; Izmaylov, A.F.; Bloino, J.; Zheng, G.; Sonnenberg, J.L.; Hada, M.; Ehara, M.; Toyota, K.; Fukuda, R.; Hasegawa, J.; Ishida, M.; Nakajima, T.; Honda, Y.; Kitao, O.; Nakai, H.; Vreven, T.; Montgomery, J.A., Jr; Peralta, J.E.; Ogliaro, F.; Bearpark, M.; Heyd, J.J.; Brothers, E.; Kudin, K.N.; Staroverov, V.N.; Kobayashi, R.; Normand, J.; Raghavachari, K.; Rendell, A.; Burant, J.C.; Iyengar, S.S.; Tomasi, J.; Cossi, M.; Rega, N.; Millam, J.M.; Klene, M.; Knox, J.E.; Cross, J.B.; Bakken, V.; Adamo, C.; Jaramillo, J.; Gomperts, R.; Stratmann, R.E.; Yazyev, O.; Austin, A.J.; Cammi, R.; Pomelli, C.; Ochterski, J.W.; Martin, R.L.; Morokuma, K.; Zakrzewski, V.G.; Voth, G.A.; Salvador, P.; Dannenberg, J.J.; Dapprich, S.; Daniels, A.D.; Farkas, O.; Foresman, J.B.; Ortiz, J.V.; Cioslowski, J.; Fox, D.J. *GAUSSIAN 09 (Revision C.01)*; Gaussian Inc.: Wallingford, CT, **2009**.

[12] Becke, A.D. Density-functional exchange-energy approximation with correct asymptotic behavior. *Phys. Rev. A Gen. Phys.,* **1988**, *38*(6), 3098-3100. [http://dx.doi.org/10.1103/PhysRevA.38.3098] [PMID: 9900728]

[13] Lee, C.; Yang, W.; Parr, R.G. Development of the Colle-Salvetti correlation-energy formula into a functional of the electron density. *Phys. Rev. B Condens. Matter,* **1988**, *37*(2), 785-789. [http://dx.doi.org/10.1103/PhysRevB.37.785] [PMID: 9944570]

[14] *GaussView 5.0*; Gaussian Inc.: Carnegie Office Park, Pittsburgh, PA, USA., **1988**.

[15] Anantha Lakshmi, P.V.; Reddy, P.S.; Raju, V.J. Synthesis, characterization and antimicrobial activity of 3d transition metal complexes of a biambidentate ligand containing quinoxaline moiety. *Spectrochim. Acta A Mol. Biomol. Spectrosc.,* **2009**, *74*(1), 52-57. [http://dx.doi.org/10.1016/j.saa.2009.05.007] [PMID: 19539520]

[16] Saravanamoorthy, S.; Velmathi, S. Transition metal complexes of tridentate Schiff base ligand as efficient reusable catalyst for the synthesis of polycaprolactone and polylactide. *Ind. J.Chem.,* **2016**, *55*, 344-352.

[17] Ekmekcioglu, P.; Karabocek, N.; Karabocek, S.; Emirik, M. Synthesis, structural and biochemical activity studies of a new hexadentate Schiff base ligand and its Cu(II), Ni(II), and Co(II) complexes. *J. Mol. Struct.,* **2015**, *1099*, 189-196. [http://dx.doi.org/10.1016/j.molstruc.2015.06.051]

[18] Mir, J.M.; Rajak, D.K.; Maurya, R.C. Bacterial sensitivity and SOD behavior of N-pyrone glucosamine Schiff base Fe(III) complex: conjoint experimental-DFT evaluation. *J. Coord. Chem.,* **2017**, *70*(18), 3199-3216. [http://dx.doi.org/10.1080/00958972.2017.1374381]

[19] Bardakçı, T.; Kumru, M.; Altun, A. Molecular structures, charge distributions, and vibrational analyses of the tetracoordinate Cu(II), Zn(II), Cd(II), and Hg(II) bromide complexes of *p*-toluidine investigated by density functional theory in comparison with experiments. *J. Mol. Struct.,* **2016**, *1116*, 292-302. [http://dx.doi.org/10.1016/j.molstruc.2016.03.023]

[20] Shukla, S.N.; Gaur, P.; Bagri, S.S.; Mehrotra, R.; Chaurasia, B.; Raidas, M.L. Pd(II) complexes with ONN pincer ligand: Tailored synthesis, characterization, DFT, and catalytic activity toward the Suzuki-Miyaura reaction. *J. Mol. Struct.,* **2021**, *1225*, 129071. [http://dx.doi.org/10.1016/j.molstruc.2020.129071]

[21] Rajaei, I.; Mirsattari, S.N. Synthesis and spectroscopic properties of a

copper(II) binuclear complex of a novel tetradentate asymmetrical Schiff base ligand and its DFT study. *Polyhedron,* **2015**, *102*, 479-489. [http://dx.doi.org/10.1016/j.poly.2015.10.019]

[22] Geary, W.J. The use of conductivity measurements in organic solvents for the characterisation of coordination compounds. *Coord. Chem. Rev.,* **1971**, *7*(1), 81-122. [http://dx.doi.org/10.1016/S0010-8545(00)80009-0]

[23] Mehrotra, R.; Shukla, S.N.; Gaur, P. Spectroscopic characterization of Schiff base coordinating monomolecular trinuclear complexes prepared through tailored synthesis. *J. Coord. Chem.,* **2012**, *65*(1), 176-190. [http://dx.doi.org/10.1080/00958972.2011.645814]

[24] Rai, N.; Mehrotra, R.; Gaur, P.; Shukla, S.N. Pyrolytic synthesis of metal sulphide quantum dots from 1-((thiophen-2-yl)methylene) thiosemicarbazide complexes and their application in catalysis. *Top. Catal.,* **2022**. [http://dx.doi.org/10.1007/s11244-022-01573-x]

[25] Chaudhary, N.K.; Mishra, P. Bioactivity of some divalent M(II) complexes of penicillin based Schiff base ligand: Synthesis, spectroscopic characterization, and thermal study. *J. Saudi Chem. Soc.,* **2018**, *22*(5), 601-613. [http://dx.doi.org/10.1016/j.jscs.2017.10.003]

[26] Warad, I.; Khan, A.A.; Azam, M.; Al-Resayes, S.I.; Haddad, S.F. Design and structural studies of diimine/CdX2 (X=Cl, I) complexes based on 2,2-dimethyl-1,3-diaminopropane ligand. *J. Mol. Struct.,* **2014**, *1062*, 167-173. [http://dx.doi.org/10.1016/j.molstruc.2014.01.001]

[27] Mehrotra, R.; Shukla, S.N.; Gaur, P. Promising trend for amendment of drug molecule against resist pathogens: synthesis, characterization, and application. *Med. Chem. Res.,* **2012**, *21*(12), 4455-4462. [http://dx.doi.org/10.1007/s00044-012-9986-0]

[28] Miessler, G.L.; Donald, A.T. *Inorganic Chemistry,* 3rd; Pearson Prentice Hall, **2008**, pp. 1-706.

[29] Chung, J.Y.; Schulz, C.; Bauer, H.; Sun, Y.; Sitzmann, H.; Auerbach, H.; Pierik, A.J.; Schünemann, V.; Neuba, A.; Thiel, W.R. Cyclopentadienide Ligand Cp^{C-} possessing intrinsic helical chirality and its ferrocene analogues. *Organometallics,* **2015**, *34*(22), 5374-5382. [http://dx.doi.org/10.1021/acs.organomet.5b00673]

[30] Mehrotra, R.; Shukla, S.N.; Gaur, P.; Rai, N. Systematic evaluation of lipophilicity in correlation with pharmacophore identification to develop potent bacterial inhibitors. *Chemistry Africa,* **2019**, *2*(4), 625-634. [http://dx.doi.org/10.1007/s42250-019-00078-7]